AAS 15-695

OPTIMAL LOW THRUST ORBIT CORRECTION IN CURVILINEAR COORDINATES

Juan L. Gonzalo*, and Claudio Bombardelli†

The minimum-time, constant-thrust transfer between two close, coplanar, quasi-circular orbits is studied using a novel non-linear formulation of relative motion in curvilinear coordinates. The Optimal Control Problem in the thrust orientation angle is treated from a quantitative and qualitative point of view, using the direct and indirect methods respectively. The former yields numerical solutions for a wide range of thrust parameters, while a better understanding of the physics is achieved seeking for an approximate solution of the latter. Fundamental changes in the structure of the solution with the thrust parameter are identified.

INTRODUCTION

Many operational scenarios require to perform small corrections in the radius and phasing of an orbit, using either impulsive or continuous low-thrust propulsion. A relatively new and challenging application for such maneuvers is the design of Active Debris Removal missions, where the chaser spacecraft must be placed in the same orbit as the target debris and at a prescribed operational distance. The former condition is normally not met by the initial orbit of the chaser, especially when launched as a piggyback payload or when a multiple target mission is considered, requiring an orbit correction. Furthermore, a precise phasing maneuver is also needed to fulfill the normally tight margins for the operational distance. These mission design issues have a prominent importance in LEOSWEEP (improving LEO Security With Enhanced Electric Propulsion),[1] an EU-funded project aiming at the contactless manipulation of non-cooperative targets using modified electric thrusters.[2]

This type of proximity rendezvous maneuvers were studied in the classical book by Marec,[3] obtaining closed solutions only for a small set of conditions. Its remarkable complexity has been further highlighted by the work of authors such as Hall and Collazo-Perez,[4] who identified qualitative changes in the minimum-time orbit phasing maneuver depending on the magnitude of thrust. The more complex problem of designing low-thrust reconfiguration maneuvers for spacecraft in formation flying subjected to multiple operational constraints has been studied in detail by Massari and Bernelli-Zazzera,[5] who propose an efficient algorithm implementation to cope with the increased computational cost of optimizing the trajectories of several spacecraft simultaneously. In all cases, an appropriate choice of the dynamics formulation can ease their treatment to a great extent. The key idea behind this article it to employ a novel relative motion formulation based on curvilinear coordinates. It can be seen as a continuation of the work already carried out by this authors using the Clohessy-Wiltshire equations for relative motion[6] aiming to improve the previous results both in precision and validity range.

*PhD candidate, Space Dynamics Group, School of Aerospace Engineering, Technical University of Madrid (UPM).
†Research Associate, Space Dynamics Group, School of Aerospace Engineering. Technical University of Madrid (UPM).

In this work, the minimum-time proximity rendezvous maneuver between two close, coplanar, quasi-circular orbits is studied from a qualitative and quantitative point of view. A non-linear formulation in curvilinear coordinates is used to describe relative dynamics, and the Optimal Control Problem in the thrust angle orientation is posed using both the direct and indirect formulations. The former leads to a set of numerical solutions, while the latter provides more insight on the underlying physics. While the focus is set in low-thrust transfers, a wide rage for the thrust parameter is considered.

The formulation used for the relative motion differs from the classical solution by Clohessy and Wiltshire in two aspects. On the one hand, it introduces curvilinear coordinates to achieve a better description of the natural orbit curvature. On the other hand, it takes into account nonlinear terms to improve accuracy when initial velocity and displacement conditions are not very small. Nevertheless, the limitation of initially circular orbit still applies.

A qualitative understanding of the problem is sought for first by studying the Two-Point Boundary Value Problem (TPVBP) derived from the Euler-Lagrange equations. The approximate analytical solutions obtained for this TPBVP using perturbation techniques predict the existence of two different regimes with fundamental qualitative differences depending on the ratio between the desired displacement and the available thrust. A direct relation between mission time and thrust is also identified for both regimes. This is in line with the previous works already mentioned.[4,6] Moreover, the approximate solutions also provide fast tools to predict some of their most notable features such as the location of the transition between both regimes and the mission time. These predictions are then compared with the high-precision numerical solutions obtained using a direct transcription method and a large-scale Non-Linear Programming solver, finding a great agreement between them. While the authors have already studied this kind of behaviors for the same-orbit rephasing problem using the Clohessy-Wiltshire equations for relative motion,[6] the introduction of this novel formulation for orbital dynamics allows for a more precise description of the problem with a wider validity range.

PROBLEM STATEMENT AND EQUATIONS OF MOTION

Let us consider two objects, a leader L and a chaser C, describing two close, coplanar, circular orbits of radii R and r around a primary O with gravitational constant μ. The objective is to perform a rendezvous maneuver, placing the chaser in the same orbit as the leader at a given angular separation. The propellant mass expelled from the chaser m_{prop} is assumed to be negligible compared to its total mass m_C, so the later can be taken as constant. From now on, all the equations and variables will be expressed in non-dimensional form, taking

$$R\ , \qquad \Omega^{-1} = \sqrt{\frac{R^3}{\mu}}\ , \qquad m_C \tag{1}$$

as the characteristic magnitudes for length, time and mass respectively.

Dynamics will be studied using a non-linear relative motion formulation in curvilinear coordinates.[7] Let us begin by introducing a Local Vertical-Local Horizontal (LVLH) reference frame centered at the leader $\mathcal{F} = \{L; \mathbf{i}', \mathbf{j}', \mathbf{k}'\}$ as shown in Figure 1. The position and velocity of the follower can be written as:

$$\mathbf{r} = x\mathbf{i}' + y\mathbf{j}' + z\mathbf{k}'$$
$$\mathbf{v} = \dot{x}\mathbf{i}' + \dot{y}\mathbf{j}' + \dot{z}\mathbf{k}'$$

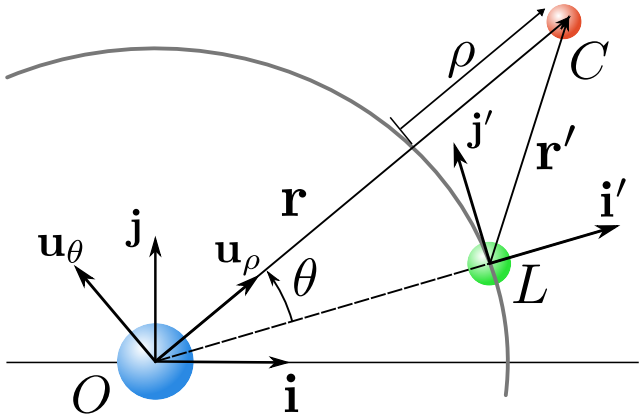

Figure 1. Schematic representation of the problem.

The curvilinear coordinates ρ and θ are now defined in the form

$$\rho = -1 + \sqrt{(x+1)^2 + y^2}\,, \quad \theta = \operatorname{atan2}(y, 1+x)$$
$$x = -1 + (1+\rho)\cos\theta\,, \quad y = (1+\rho)\sin\theta$$

where θ is the angle formed by the position vectors of chaser and leader, and ρ is the radial separation of the chaser from the orbit of the leader. Projecting the equations of motion along the radial and transversal unity vectors

$$\mathbf{u}_\rho = \cos\theta\mathbf{i}' + \sin\theta\mathbf{j}'$$
$$\mathbf{u}_\theta = -\sin\theta\mathbf{i}' + \cos\theta\mathbf{j}'$$

as well as the normal unity vector, one finally reaches

$$\begin{aligned} \ddot{\rho} - 2\dot{\theta} - 3\rho &= a_{i\rho} + a_{g\rho} + a_{T\rho} \\ \ddot{\theta} + 2\dot{\rho} &= a_{i\theta} + a_{T\theta} \\ \ddot{z} + z &= a_{gz} + a_{Tz} \end{aligned} \tag{2}$$

where $a_{i\rho}$, $a_{g\rho}$, $a_{i\theta}$ and a_{gz} account for the non-linear perturbation terms

$$a_{i\rho} = \dot{\theta}^2(1+\rho) + 2\dot{\theta}\rho\,, \quad a_{i\theta} = \frac{2\dot{\rho}\left(\rho - \dot{\theta}\right)}{1+\rho}\,,$$

$$a_{g\rho} = -2\rho + 1 - \frac{1+\rho}{\left[(1+\rho)^2 + z^2\right]^{3/2}}\,, \quad a_{gz} = z - \frac{z}{\left[(1+\rho)^2 + z^2\right]^{3/2}}\,,$$

while $a_{T\rho}$, $a_{T\theta}$ and a_{Tz} correspond to the actions of the continuous-thrust engine.

Restricting ourselves to the planar case, the previous equations read

$$\begin{aligned} \ddot{\rho} - 2\dot{\theta} - 3\rho &= a_{i\rho} + a_{g\rho} + a_{T\rho} \\ \ddot{\theta} + 2\dot{\rho} &= a_{i\theta} + a_{T\theta} \end{aligned} \tag{3}$$

with

$$a_{T\rho} = \varepsilon \sin\gamma \quad , \qquad a_{T\theta} = \varepsilon \cos\gamma$$

where ε is the non-dimensional magnitude of the thrust acceleration, and γ is its orientation with respect to the transversal direction. Introducing the state vector

$$\mathbf{S} = \left[\begin{array}{cccc} \dot{\rho} & \dot{\theta} & \rho & \theta \end{array} \right]^\top \tag{4}$$

the equations can be expressed as a first order system in the form

$$\frac{\mathrm{d}\mathbf{S}}{\mathrm{d}\tau} = \mathbf{F}\left(\tau, \mathbf{S}\right) \ , \quad \text{with} \quad \mathbf{F}\left(\tau, \mathbf{S}\right) = \left[\begin{array}{c} 2\dot{\theta} + 3\rho + a_{i\rho} + a_{g\rho} + a_{T\rho} \\ -2\dot{\rho} + a_{i\theta} + a_{T\theta} \\ \dot{\rho} \\ \dot{\theta} \end{array} \right] , \tag{5}$$

where τ is the non-dimensional time.

Neglecting the non-linear perturbing terms, a linear formulation with the same structure as the Clohessy-Wiltshire equations is reached:

$$\begin{aligned} \ddot{\rho} - 2\dot{\theta} - 3\rho &= a_{T\rho} \\ \ddot{\theta} + 2\dot{\rho} &= a_{T\theta} \end{aligned} \tag{6}$$

or as a first order system:

$$\frac{\mathrm{d}\mathbf{S}}{\mathrm{d}\tau} = \mathbf{F}^*\left(\tau, \mathbf{S}\right) \ , \quad \text{with} \quad \mathbf{F}^*\left(\tau, \mathbf{S}\right) = \left[\begin{array}{c} 2\dot{\theta} + 3\rho + a_{T\rho} \\ -2\dot{\rho} + a_{T\theta} \\ \dot{\rho} \\ \dot{\theta} \end{array} \right] . \tag{7}$$

The final state for the proposed rendezvous maneuver must enforce that the chaser reaches the same orbit as the leader with a certain phasing, leading to

$$\mathbf{S}\left(\tau_f\right) = \left[\begin{array}{cccc} \dot{\rho}_f & \dot{\theta}_f & \rho_f & \theta_f \end{array} \right]^\top = \left[\begin{array}{cccc} 0 & 0 & 0 & \theta_f \end{array} \right]^\top .$$

On the other hand, the initial state is determined by the original orbit of the chaser

$$\mathbf{S}\left(\tau_0\right) = \left[\begin{array}{cccc} \dot{\rho}_0 & \dot{\theta}_0 & \rho_0 & \theta_0 \end{array} \right]^\top = \left[\begin{array}{cccc} 0 & \sqrt{1/(\rho_0+1)^3} - 1 & -\Delta\rho & \theta(\tau_0) \end{array} \right]^\top .$$

where $\dot{\theta}_0$ comes from imposing initially circular orbit, $\Delta\rho = \rho_f - \rho_0 = -\rho_0$ is the desired radial displacement, and θ_0 is set free. The latter implies that the phasing problem will be solved by simply selecting the angular position at which the maneuver is started, which is a fuel-efficient solution for LEO orbits, separating it from the radius modification problem. Furthermore, without loss of generality we can set $\theta_f = 0$, and the boundary conditions take the final form:

$$\begin{aligned} \mathbf{S}\left(\tau_f\right) &= \left[\begin{array}{cccc} 0 & 0 & 0 & 0 \end{array} \right]^\top \\ \mathbf{S}\left(\tau_0\right) &= \left[\begin{array}{cccc} 0 & \sqrt{1/(\rho_0+1)^3} - 1 & -\Delta\rho & -\Delta\theta \end{array} \right]^\top , \end{aligned} \tag{8}$$

with $\Delta\theta = \theta_f - \theta_0 = -\theta_0$.

CONTINUOUS THRUST MANEUVER

The minimum-time transfer between two close, coplanar, circular orbits is now studied for the continuous, constant thrust case, using both the indirect and direct formulations. The solutions are not restricted to low-thrust, covering a wide range of values for the non-dimensional thrust parameter. Furthermore, since the mass of the maneuvering spacecraft has been assumed to be constant, this Optimal Control Problem (OCP) is equivalent to minimizing the total impulse required for the transfer.

The indirect method is considered first, posing the Two Point Boundary Value Problem derived from the first order optimality conditions and studying it from a qualitative point of view. Although it is not possible to obtain closed analytical solutions, and we have restricted the numerical treatment of the OCP to the direct method, several key conclusions about the structure of the problem are reached, identifying two different regimes depending on the ratio between radial displacement and thrust parameter, and giving a first estimate of the maneuver time.

The OCP is then solved numerically using the direct method, for several values of the radial displacement and the thrust parameter. The results confirm the conclusions from the previous qualitative analysis, and expand the information about those cases where the analytical approximations where not valid.

Indirect Method

The cost function for a minimum-time maneuver can be expressed in the form:[8]

$$J = \int_0^{\tau_f} L\left(\mathbf{S}, \gamma, \tau\right) \mathrm{d}\tau \, = \tau_f$$

where $L\left(\mathbf{S}, \gamma, \tau\right) = 1$ is the Lagrangian, and there is no dependence of the cost function with the final state. Introducing a costate $\boldsymbol{\lambda}$, the Hamiltonian is then defined as:

$$H = \boldsymbol{\lambda}^\top \cdot \mathbf{F} + L \quad , \qquad \boldsymbol{\lambda}^\top = \left[\begin{array}{cccc} \lambda_{\dot{\rho}} & \lambda_{\dot{\theta}} & \lambda_\rho & \lambda_\theta \end{array} \right]^\top . \tag{9}$$

The solution to the OCP can now be obtained by imposing the first order optimality conditions given by the Euler-Lagrange equations. Using the Hamiltonian previously defined, one reaches four adjoint equations

$$\dot{\boldsymbol{\lambda}} = -\frac{\partial H}{\partial \mathbf{S}} \, , \tag{10}$$

one control equation

$$0 = \frac{\partial H}{\partial \gamma} \Rightarrow 0 = \varepsilon \lambda_{\dot{\rho}} \cos\gamma - \varepsilon \lambda_{\dot{\theta}} \sin\gamma \, , \tag{11}$$

and one transversality condition, introduced by the minimum-time requirement

$$H\left(\tau_f\right) = 0 \Rightarrow \boldsymbol{\lambda}^\top \cdot \mathbf{F}\Big|_{\tau_f} = -1 \, , \tag{12}$$

which along the equations of motion yield a Two-Point Boundary Value Problem (TPVBP), formed by eight differential Equations (5) and (10), and two algebraic Equations (11) and (12). The boundary conditions for this TPVBP are imposed either on the state or its corresponding costate, so that the boundary value of an element of the costate associated to a fixed element of the state is free,

while each element of the costate associated to a terminally-free element of the state must have a boundary value of 0. From the boundary conditions of the problem, Eq. (8):

$$\dot{\rho}\left(\tau_0\right)=0\,,\quad \dot{\theta}\left(\tau_0\right)=\dot{\theta}_0\,,\quad \rho\left(\tau_0\right)=-\Delta\rho\,,\quad \lambda_\theta\left(\tau_0\right)=0$$
$$\dot{\rho}\left(\tau_f\right)=0\,,\quad \dot{\theta}\left(\tau_f\right)=0\,,\quad \rho\left(\tau_f\right)=0\,,\quad \theta\left(\tau_f\right)=0$$

The previous TPBVP cannot be solved analytically for a general case. A numerical solution could be sought for using several algorithms such as shooting methods, but as previously stated the numerical part of this study is focused on the direct method. Instead, the TPVBP is now studied from a qualitative point of view, with the aim to extract knowledge about the structure of the solution and the evolution of the state. This information can then be used to generate initial guesses for the iterative Non-Linear Programming algorithms used in the direct method.

To ease the treatment of the equations, the linearized formulation of the relative motion in curvilinear coordinates is used. This leads to the following set of adjoint equations:

$$\begin{aligned}\dot{\lambda}_{\dot{\rho}}&=-\lambda_\rho+2\lambda_{\dot{\theta}}\\ \dot{\lambda}_{\dot{\theta}}&=-2\lambda_{\dot{\rho}}-\lambda_\theta\\ \dot{\lambda}_\rho&=-3\lambda_{\dot{\rho}}\\ \dot{\lambda}_\theta&=0\end{aligned}$$

Note that, by neglecting the non-linear terms, the adjoint equations have been decoupled from the equations of motion. The solution for these linearized adjoint equations along with the boundary condition $\lambda_\theta\left(\tau_0\right)=0$ is now straightforward

$$\begin{aligned}\lambda_{\dot{\rho}}&=A\sin\left(\tau+\varphi\right)\\ \lambda_{\dot{\theta}}&=2A\cos\left(\tau+\varphi\right)+B\\ \lambda_\rho&=3A\cos\left(\tau+\varphi\right)+2B\\ \lambda_\theta&=0\end{aligned}$$

Since only one boundary condition is given for the costate, the solution depends on three parameters which would be determined by imposing the boundary conditions for the state. It is observed that the costate for θ is equal to zero in all cases; this is due to the fact that θ is subjected to no constraints during the maneuver. This will also hold true for the non-linear case.

Control Eq. (11) allows to express the thrust orientation angle γ as a function of the costate, leading to the following expressions

$$\sin\gamma=-\mathrm{sgn}\left(\varepsilon\right)\frac{\lambda_{\dot{\rho}}}{\sqrt{\lambda_{\dot{\rho}}^2+\lambda_{\dot{\theta}}^2}}\,,\quad \cos\gamma=-\mathrm{sgn}\left(\varepsilon\right)\frac{\lambda_{\dot{\theta}}}{\sqrt{\lambda_{\dot{\rho}}^2+\lambda_{\dot{\theta}}^2}}\,,$$
$$\gamma=\mathrm{atan2}\left(-\mathrm{sgn}\left(\varepsilon\right)\lambda_{\dot{\rho}},-\mathrm{sgn}\left(\varepsilon\right)\lambda_{\dot{\theta}}\right)\,.$$

Finally, introducing the known values of the final state into the transversality condition for optimum final time, Eq. (12), yields

$$\lambda_{\dot{\rho}}\varepsilon\sin\gamma+\lambda_{\dot{\theta}}\varepsilon\cos\gamma+1\big|_{\tau_f}=0\,,$$

and substituting the previous expressions for $\sin\gamma$ and $\cos\gamma$:

$$\lambda_{\dot{\rho}}(\tau_f)^2+\lambda_{\dot{\theta}}(\tau_f)^2=\frac{1}{\varepsilon^2}\,. \tag{13}$$

So far, the original TPVBP has been reduced from eight ODEs and two algebraic conditions to the four linearized equations of motion, Eqs. (7), and one algebraic condition, Eq. (13), with five unknowns τ_f, A, B, φ and θ_0. However, there is no closed solution for the linearized equations of motion perturbed by a continuous thrust acceleration, so it is not possible to find a fully analytical solution for the OCP even in the linearized case. Nevertheless, additional information on the solution can be obtained by analyzing the orders of magnitude of the different terms in the equations and locating the dominant ones. To this end, the linear, second order equations of motion are considered:

$$\underbrace{\frac{\mathrm{d}^2\rho}{\mathrm{d}\tau^2}}_{\frac{\Delta\rho}{\Delta\tau^2}} = \underbrace{2\frac{\mathrm{d}\theta}{\mathrm{d}\tau}}_{2\frac{\Delta\theta}{\Delta\tau}} + \underbrace{3\rho}_{3\Delta\rho} + \underbrace{\varepsilon\sin\gamma}_{\varepsilon u_\rho} \quad , \qquad \underbrace{\frac{\mathrm{d}^2\theta}{\mathrm{d}\tau^2}}_{\frac{\Delta\theta}{\Delta\tau^2}} = -\underbrace{2\frac{\mathrm{d}\rho}{\mathrm{d}\tau}}_{2\frac{\Delta\rho}{\Delta\tau}} + \underbrace{\varepsilon\cos\gamma}_{\varepsilon u_\theta} \tag{14}$$

with

$$\begin{aligned}
&\Delta\rho = \rho_f - \rho_0 = -\rho_0 \\
&\Delta\theta = \theta_f - \theta_0 = -\theta_0 \\
&\Delta\tau = \tau_f - \tau_0 = \tau_f \\
&|u_\rho|, |u_\theta| \leq 1
\end{aligned}$$

Note that $\Delta\rho$ has a fixed value imposed by the requirements of the maneuver, while $\Delta\theta$ is a free parameter. According to the second of Eqs. (14), said angular displacement can be driven both by gravitational effects and the action of thrust. Considering the case where thrust is dominant, it is possible to write:

$$\Delta\theta \sim \varepsilon\tau_f^2 u_\theta$$

and introducing it into the first equation yields the following orders of magnitude

$$\Delta\rho \quad \varepsilon\tau_f^3 u_\theta \quad 3\Delta\rho\tau_f^2 \quad \varepsilon\tau_f^2 u_\rho$$

For long non-dimensional mission times $\tau_f \gg 1$, the second and third terms are dominant, leading to

$$\tau_f \sim \frac{\Delta\rho}{\varepsilon u_\theta}$$

which not only gives a first estimate of the required maneuver time, but also shows that the optimum thrust orientation profile will remain close to the transversal direction. For the short mission time scenario $\tau_f \ll 1$, the first and fourth terms become dominant (note that at least one control term must be retained), giving the following estimate for the maneuver time:

$$\tau_f \sim \sqrt{\frac{\Delta\rho}{\varepsilon u_\rho}}$$

Interestingly, the preferred orientation of thrust for minimum time maneuvers has changed from the transversal to the radial direction.

Carefully examining these two regimes, it is possible to check that the gravity-dominated scenario is already included in them. Certainly, for long maneuver times introducing the expression for τ_f into the second equation yields

$$\Delta\theta \quad \frac{\Delta\rho^2}{\varepsilon u_\theta} \quad \frac{\Delta\rho^2}{\varepsilon u_\theta}$$

showing that both gravitational and thrust effects are of the same order, and giving an estimate for $\Delta\theta$. Nevertheless, the first equation indicates that the desired displacement in ρ is reached through the coupling between both equations due to the gravitational effects, so this regime will be referred to as gravity-dominated.

In the short maneuver time case, that same equation reads

$$\Delta\theta \quad \Delta\rho\tau_f \quad \Delta\rho\frac{u_\theta}{u_\rho}$$

where the minimum-time condition of dominantly radial thrust implies that $|u_\theta| \ll 1$. Therefore, transversal control will be at most of the same order as the gravitational effects, due to the need to meet the boundary conditions in $\dot{\theta}$, yielding $u_\theta \lesssim \tau_f \ll 1$ (that is, the shorter the maneuver time the more close the thrust profile will be to the radial direction). Since the displacement in ρ is mainly driven by the action of thrust in its direction, this regime will be called thrust-dominated.

The transition between both regimes takes place for

$$\tau_f \sim \mathcal{O}(1) \;\Rightarrow\; \Delta\rho \approx \varepsilon\,.$$

In this transition zone, all terms in both equations became of the same order, and no simplifications can be made. Thrust will no longer have a preferred orientation, taking intermediate positions as it evolves from one limit case to the other. Since $\tau_f = 2\pi$ corresponds to one orbital revolution of the leader, it follows that another key difference between both regimes is whether the maneuver requires less than one revolution to complete or several.

The equations of motion could be approximately solved for both regimes by neglecting the non-dominant terms, leading to a set of simplified equations. In the long maneuver time, or gravity-dominated, case, the control and acceleration terms in the radial equation become negligible compared to the other two, leading to a relation between the radial displacement and the angular velocity:

$$\frac{\mathrm{d}\theta}{\mathrm{d}\tau} = -\frac{3}{2}\rho$$

Introducing this into the second of Eqs. (14) leads to:

$$\frac{\mathrm{d}\rho}{\mathrm{d}\tau} = 2a_\theta\,.$$

Both ODEs are first order, so the boundary conditions for $\dot{\rho}$ and $\dot{\theta}$ cannot be imposed. From a physical point of view, this shows that a small component of thrust in the radial direction would be needed to enforce them. Assuming that a_θ is constant, which is consistent with the condition that thrust should be as close to the transversal direction as possible, these two equations can be solved:

$$\rho = \rho_0 + 2a_\theta\tau$$
$$\theta = \theta_0 - \frac{3}{2}\rho_0\tau - \frac{3}{2}a_\theta\tau^2$$

leading to a maneuver time

$$\tau_f = \frac{\Delta\rho}{2a_\theta} \tag{15}$$

This estimation of the maneuver time also shows that thrust must be oriented in the same sense as the velocity if the final orbit is higher than the initial one, and opposite to it if the final orbit is lower.

In the short mission time, or thrust-dominated, case, the leading terms in the radial equation are those associated with acceleration and thrust, yielding

$$\frac{\mathrm{d}^2\rho}{\mathrm{d}\tau^2} = a_\rho$$

which can be readily integrated assuming constant a_ρ

$$\begin{aligned}\dot{\rho} &= \dot{\rho}_0 + a_\rho \tau \\ \rho &= \rho_0 + \dot{\rho}_0 \tau + \frac{a_\rho}{2}\tau^2\end{aligned}$$

Introducing these results into the second of Eqs. (14)

$$\frac{\mathrm{d}^2\theta}{\mathrm{d}\tau^2} = -2\dot{\rho}_0 - 2a_\rho\tau + a_\theta$$

and integrating for constant a_ρ and a_θ

$$\begin{aligned}\dot{\theta} &= \dot{\theta}_0 + (a_\theta - 2\dot{\rho}_0)\,\tau - a_\rho\tau^2 \\ \theta &= \theta_0 + \dot{\theta}_0\tau + \frac{a_\theta - 2\dot{\rho}_0}{2}\tau^2 - \frac{a_\rho}{3}\tau^3\end{aligned}$$

The fulfillment of the final boundary condition in $\dot{\theta}$ would require a small component of thrust in the direction of θ, large enough to interact with the contribution from the main component of thrust in the direction of ρ; this leads to the already commented condition of $a_\theta \sim \tau$. Focusing on the equations for ρ, a thrust orientation profile compatible with the boundary conditions for $\dot{\rho}$ can be achieved by thrusting in one direction during the first half of the maneuver and then in the opposite direction during the second half, yielding

$$\dot{\rho}\,(\tau_f/2) = a_\rho\tau_f/2\,, \quad \dot{\rho}\,(\tau_f) = 0$$

$$\rho\,(\tau_f/2) = \rho_0 + \frac{a_\rho}{8}\tau_f^2\,, \quad \rho\,(\tau_f) = \rho\,(\tau_f/2) + \dot{\rho}\,(\tau_f/2)\,\frac{\tau_f}{2} - \frac{a_\rho}{8}\tau_f^2 = \rho_0 + \frac{a_\rho}{4}\tau_f$$

The maneuver time can now be obtained from the last equation as:

$$\tau_f = 2\sqrt{\frac{\Delta\rho}{a_\rho}} \tag{16}$$

This kind of approximate analysis cannot be carried for the transition zone, where all the terms in the equations become of comparable order. The structure of the solution undergoes fundamental qualitative changes as it moves from one regime to the other, transitioning from a nearly bang-bang thrust orientation law in the radial direction for the thrust-dominated case to approximately tangential in the gravity-dominated case. In the absence of an analytical solution for the TPVBP, this transition zone will be studied numerically using the direct method.

Direct Method

The proposed minimum-time transfer is now studied from a numerical point of view, using a direct transcription[9,10] to express the original continuous problem as a discrete Non-Linear Programing (NLP) one. This NLP subproblem is then solved using an iterative algorithm, starting from a suitable initial guess of the solution.

The discretization is performed by introducing a uniformly spaced grid of M nodes for the independent variable τ, ranging from 0 to τ_f. The optimization variable is formed by the values of the state $\mathbf{S}$ and the control γ at each node of the grid, as well as the free final time τ_f. This implies that the minimum-time objective function can be expressed as a simple function of the optimization variable

$$J = \tau_f \, .$$

The equations of motion are enforced by expressing them as a discrete set of non-linear equality constraints, called *defect constraints*, using schemes from the Implicit Runge-Kutta family.[9,11] The selection of implicit algorithms over explicit ones is based on their greater order for the same number of stages and better stability, while their normally higher computational cost is compensated by the iterative nature of the NLP algorithms. Two different schemes are considered in this study. On the one hand, the Trapezoidal Method, a 2-stages, 3^{rd} order IRK which yields $4\,(M-1)$ defect constraints, is used to obtain fast and coarse solutions. On the other hand, the Hermite-Simpson Separated (HSS) method, a 3-stages, 4^{rd} order IRK which yields $8\,(M-1)$ defect constraints, is employed to compute refined solutions. The HSS method has the additional advantage of providing information about the costate,[9] but it also presents the caveat of requiring the middle-points of the grid to be included in the optimization variable, almost doubling its size for the same number of nodes. Finally, the conditions in which the maneuver is to be performed introduce no additional path constraints, only bound constraints for the initial and final values of the state.

The NLP subproblem is solved using Ipopt (Interior Point OPTimizer), a third-party software package for large-scale nonlinear optimization.[12] It is distributed as open source code under the Eclipse Public License (EPL), and available from the COIN-OR initiative*. This NLP solver requires as an input the Jacobian of the objective function and the constraints, and can use either a user-supplied Hessian or its own limited-memory BFGS approximation. Since both the objective function and the defect constraints are relatively simple, their respective Jacobians are build analytically as sparse matrices. Regarding the Hessian, for small grids ($M \leq 200$) a numerical approximation based on finite differences of the gradients is used,[13] while the build-in L-BFGS update is preferred for larger grids. Whereas the former gives a much better approximation of the Hessian, requiring less iterations to converge and being more stable, the latter takes much less computational time to evaluate and factorize. As the size of the problem grows, the extra time spent computing and factorizing the Hessian at each step rapidly overcomes the gains from the reduced number of iterations, justifying the use of the L-BFGS approximation to improve the overall performance of the solver.

The minimum-time transfer between two coplanar, circular orbits around Earth is now computed for several values of the orbital separation and the thrust parameter. In all cases, the final orbit has an altitude of $h = 635\,\text{km}$ over Earth mean equatorial radius $R_E = 6378.1\,\text{km}$, that is

$$R = 7013.1\,\text{km}\,, \quad T_{\text{orb}} = 97.415\,\text{min}\,, \quad \Omega = 1.0750\,10^{-3}\,\text{rad/s}$$

*http://www.coin-or.org/

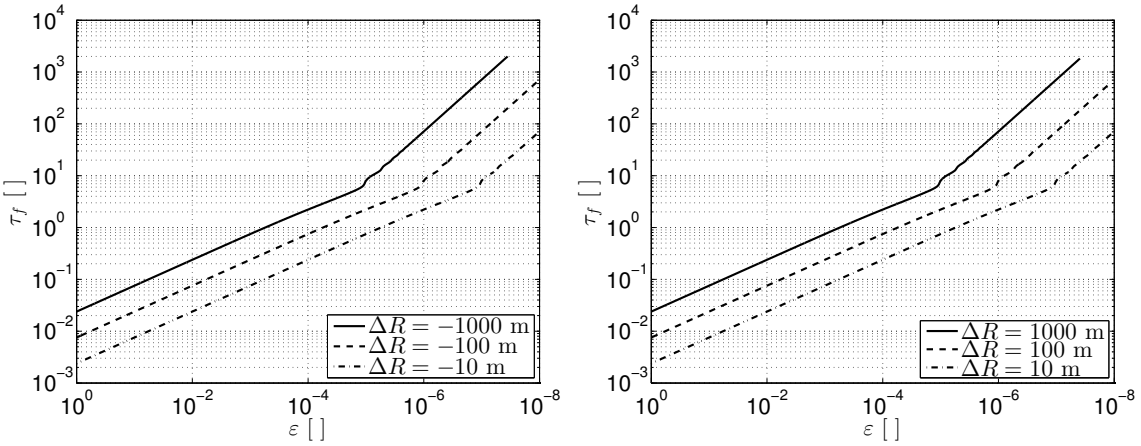

Figure 2. Time of flight as a function of the non-dimensional thrust parameter for several radial displacements.

where T_{orb} is the orbital period of the final orbit. Six different radial separations ΔR with values $\pm 10\,\text{m}$, $\pm 100\,\text{m}$ and $\pm 1000\,\text{m}$ are considered, corresponding to values of $\Delta\rho$ of $\pm 1.4259\,10^{-6}$, $\pm 1.4259\,10^{-5}$ and $\pm 1.4259\,10^{-4}$ respectively. The sign of $\Delta\rho$ indicates whether the initial orbit is above the reference orbit, negative $\Delta\rho$, or below it, positive $\Delta\rho$. A wide range of non-dimensional thrust acceleration parameters $\varepsilon \in [10^0, 10^{-8}]$ is considered, corresponding to physical accelerations between $8.1043\,\text{m/s}^2$ and $8.1043\,10^{-8}\,\text{m/s}^2$. Initial guesses are constructed either using the qualitative information obtained from the indirect method or a previous solution for the same orbital separation and a similar thrust parameter. All final solutions have been computed with the HSS method, the Trapezoidal method being used for initialization purposes only.

Figure 2 shows the evolution of the maneuver time τ_f with the non-dimensional thrust parameter ε, for different values of the radial displacement ΔR. The two different regimes predicted by the qualitative study of the equations from the indirect method can be clearly identified, with the transition between them taking place for values of τ_f around one orbit of the leader, that is, $\tau_f \approx 2\pi$. This confirms the hypothesis that one of the key differences between both regimes is whether the maneuver can be completed in one revolution or not. Interestingly, the main effect of increasing $|\Delta R|$ appears to be just a displacement of the curves along the horizontal axis; this can be clearly seen in Figure 3, where the evolution of τ_f with the ratio $\Delta\rho/\varepsilon$ is represented. While this behavior is consistent with the predictions given by the indirect method, it is important to keep in mind that those results where obtained neglecting the non linear terms in the equations of motion. Therefore, the numerical results reveal that the influence of the non-linear terms in τ_f is negligible for the considered values of the radial displacement. The predictions for τ_f obtained from the indirect method have also been represented in Figure 3, showing a great correspondence with the numerical results. The total impulse required to perform the maneuver also behaves differently in both regimes as shown by Figure 4. It decreases with maneuver time in the thrust-dominated regime, but remains nearly constant in the gravity-dominated regime. Consequently, for relatively short maneuvers (less than one revolution to complete) the required propellant can be reduced by decreasing thrust and increasing maneuver time, while for long maneuvers (more than one orbit to complete) the magnitude of thrust only has a noticeable effect in maneuver time. In all cases total impulse increases with the required radial displacement and presents the same values for orbit raising and orbit lowering maneuvers.

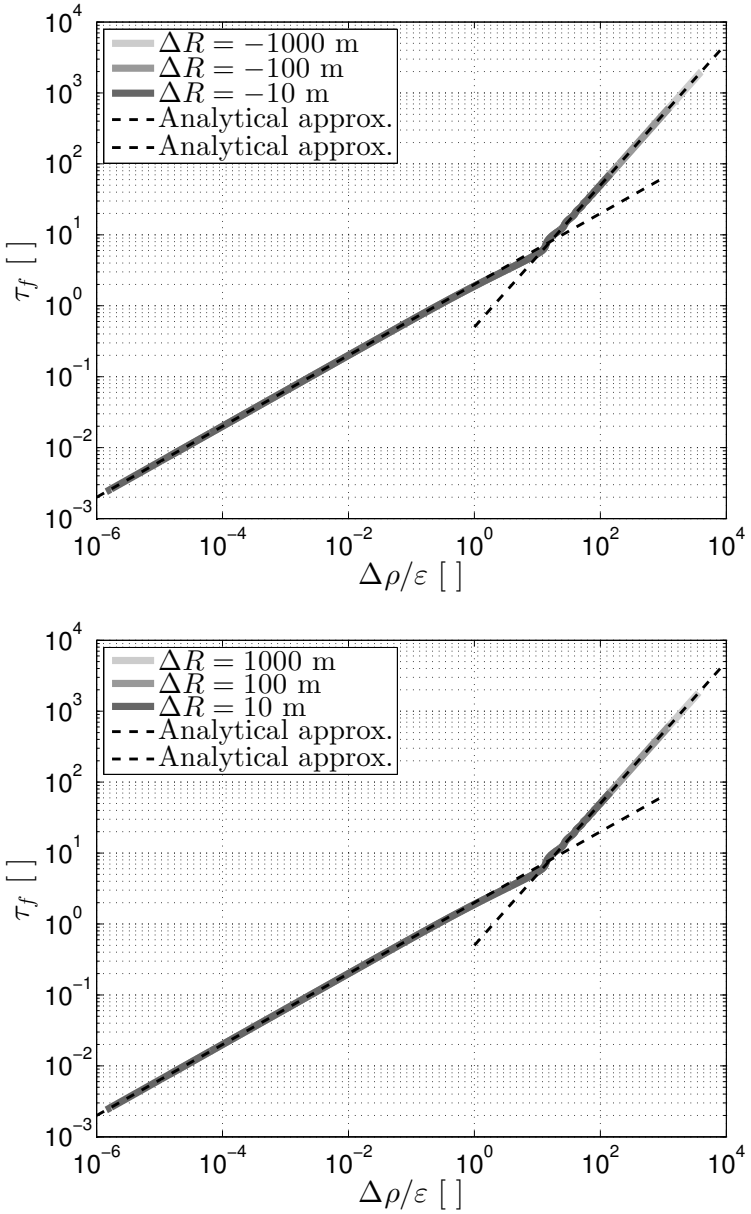

Figure 3. Time of flight as a function of the ratio between the non-dimensional radial displacement and the thrust parameter for several radial displacements.

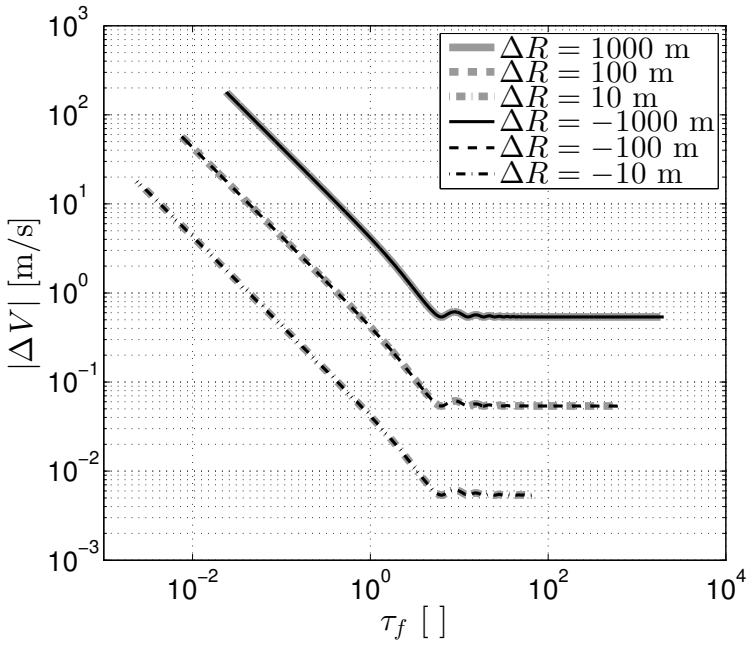

Figure 4. Total impulse in m/s as a function of non-dimensional time for several radial displacements.

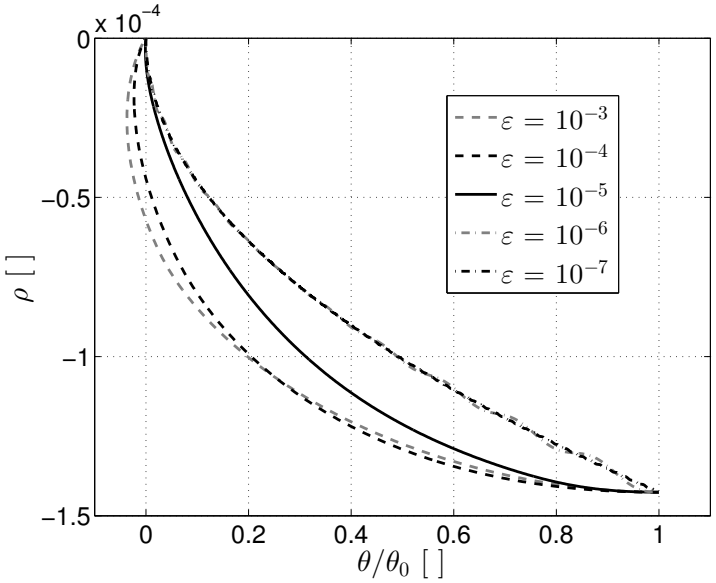

Figure 5. Minimum-time trajectories for a radial displacement of 1 km and different values of the thrust parameter.

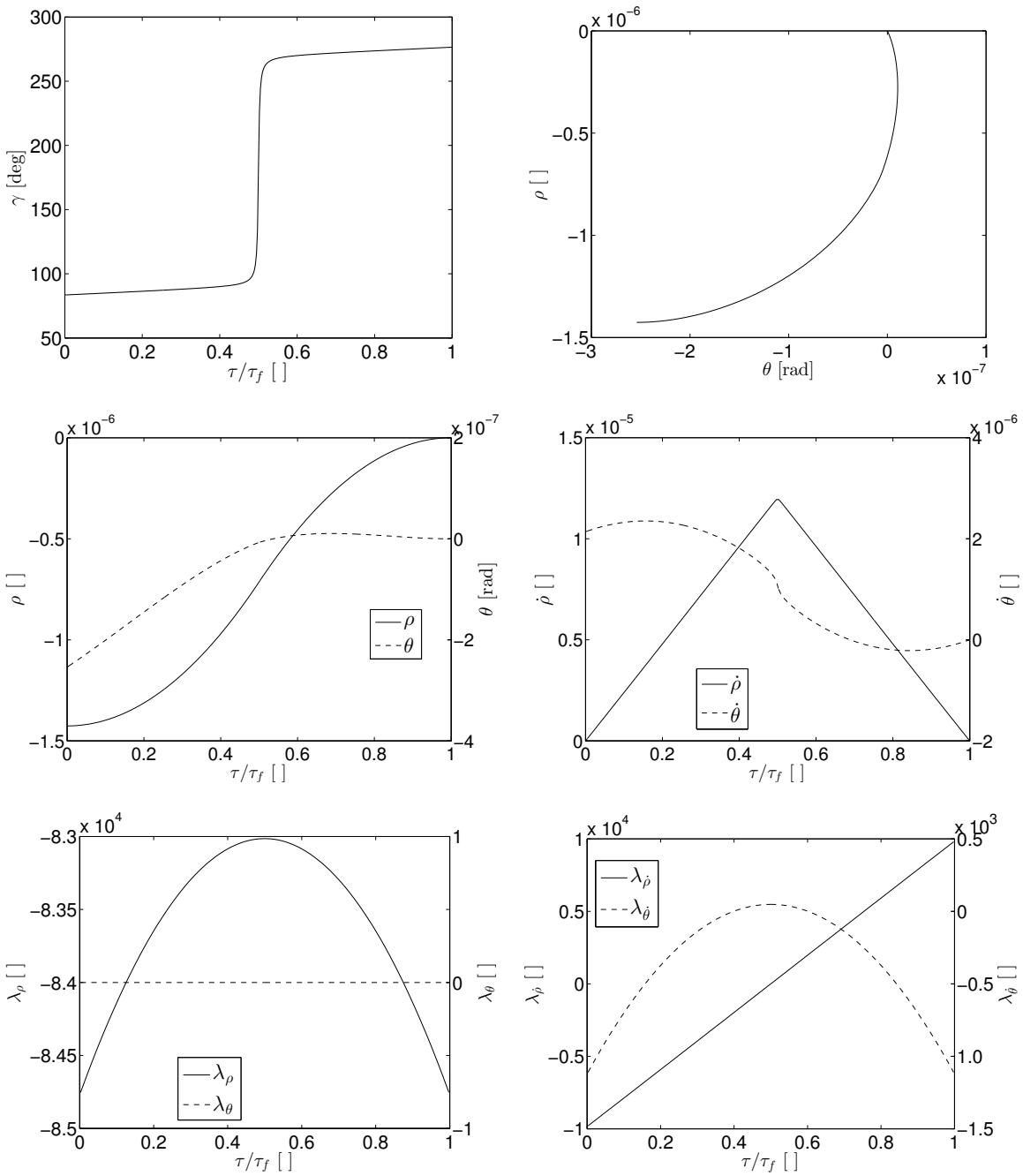

Figure 6. Minimum-time transfer for a positive radial displacement of 10 m and a non-dimensional thrust parameter of $\varepsilon = 1.0093\,10^{-4}$.

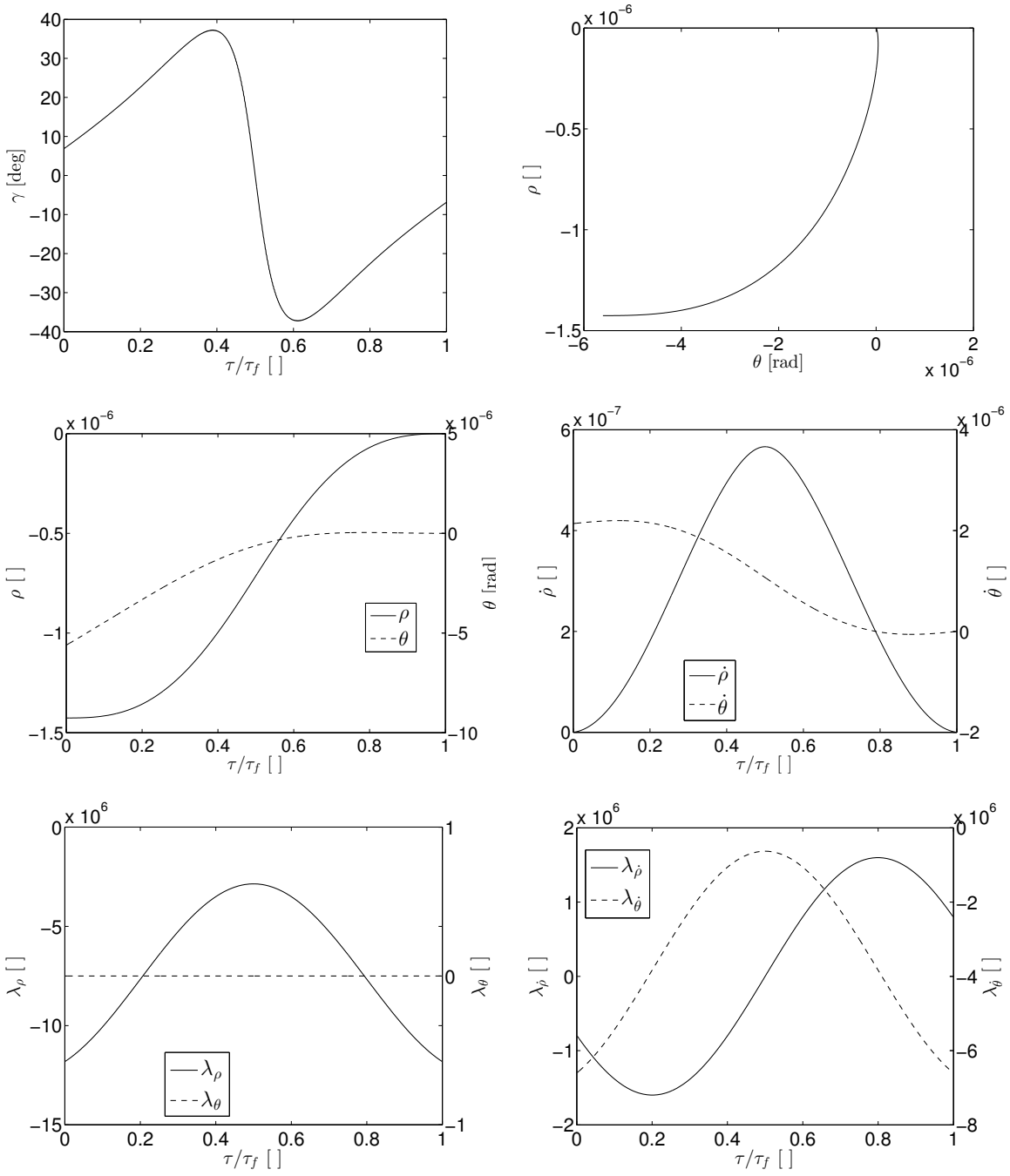

Figure 7. Minimum-time transfer for a positive radial displacement of 10 m and a non-dimensional thrust parameter of $\varepsilon = 1.5038\,10^{-7}$.

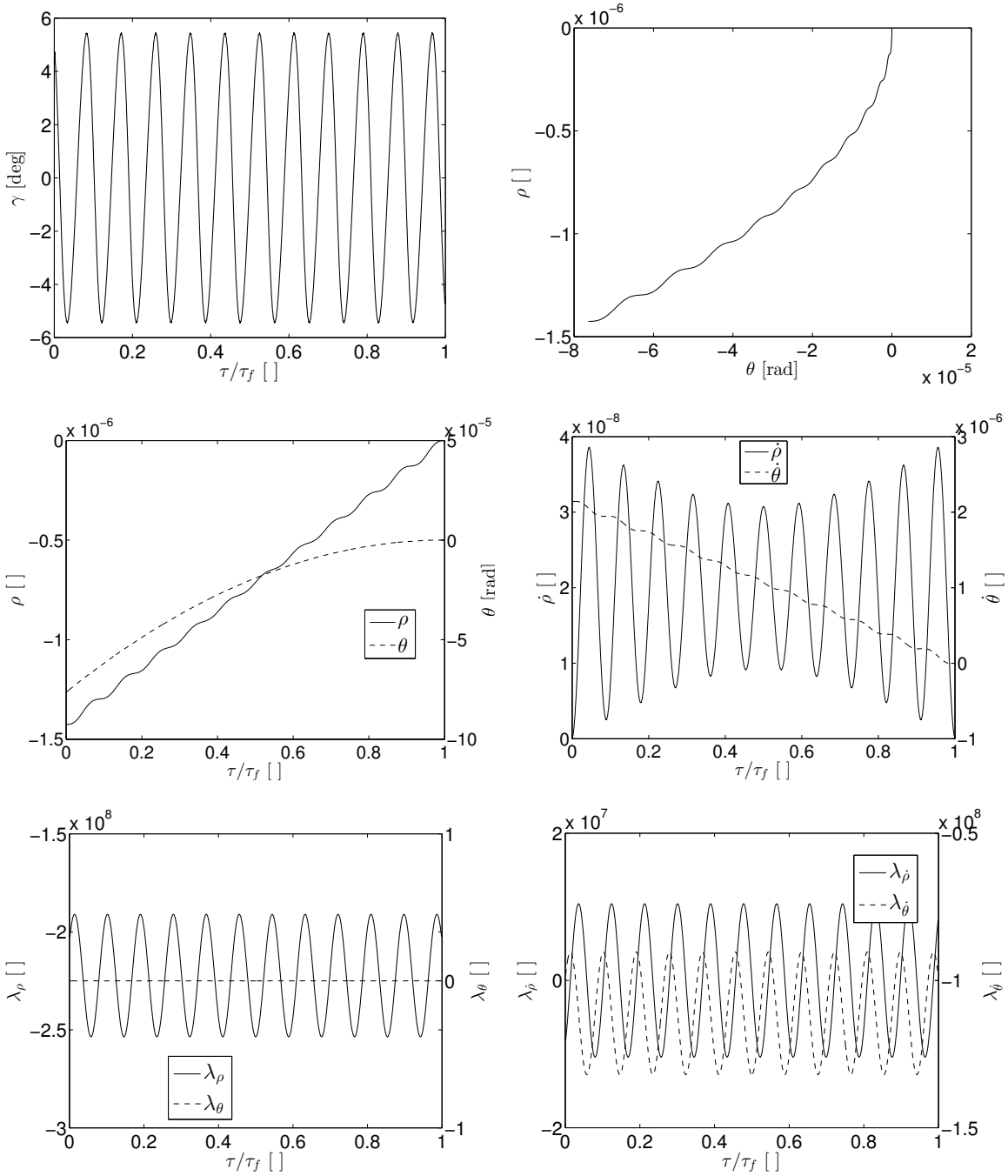

Figure 8. Minimum-time transfer for a positive radial displacement of 10 m and a non-dimensional thrust parameter of $\varepsilon = 1.0000\,10^{-8}$.

Continuing the analysis of the numerical results, Figure 5 shows the minimum-time trajectories for a radial displacement of $1\ \mathrm{km}$ and different values of ε. Since the total angular displacement strongly varies with ε, it has been normalized with its initial value to get a more clear representation of the different trajectories. The first two cases, $\varepsilon = 10^{-3}$ and $\varepsilon = 10^{-4}$, correspond to the thrust-dominated (or short mission time) regime, while the last two, $\varepsilon = 10^{-6}$ and $\varepsilon = 10^{-7}$, belong to the gravity-dominated (or long mission time) regime. The trajectory for $\varepsilon = 10^{-5}$ lies in the transition zone, separating the previous ones. It is observed that the solutions corresponding to the same regime have a very similar qualitative behavior, while drastic changes appear when moving from one regime to the other. Particularly, the thrust-dominated solutions have a distinguishable overshoot in θ and no oscillatory components, while the gravity-dominated solutions present no overshoot and small oscillations.

In order to provide a more detailed description of the problem, this section is concluded by presenting three representative cases taken from both regimes and the transition zone. All of them correspond to the same positive radial displacement of $10\,\mathrm{m}$. Figure 6 shows the thrust orientation angle, trajectory, state and costate for a solution in the thrust-dominated regime with $\varepsilon = 1.0093\,10^{-4}$, corresponding to a physical acceleration of $a = 8.1793\,10^{-4}\,\mathrm{m/s^2}$ and a maneuver time of $\tau_f = 0.2375$. The control variable γ resembles a step function, with the switch located at the middle of the maneuver. Thrust is orientated close to the positive radial direction during the first half of the maneuver, and in the second half it reverses to point opposite to it. As a consequence, the curves for $\dot{\rho}$, λ_ρ and $\lambda_{\dot{\rho}}$ are highly symmetric, while the short maneuver time prevents the gravity-dominated effects to fully develop. It is also interesting to point out that the curves for γ, ρ, $\dot{\rho}$ and the costates fit very well with the behaviors predicted by the approximate analytical study of the equations from the indirect method.

The solution has a completely different structure in the gravity-dominated regime, as shown in Figure 8 for $\varepsilon = 1.000\,10^{-8}$ ($a = 8.1043\,10^{-8}\,\mathrm{m/s^2}$, $\tau_f = 71.4536$). The thrust control angle is now oriented along the transversal direction, describing small oscillations about it. Oscillatory behaviors can also be found in the rest of variables, except for θ and λ_θ. Nevertheless, the evolution of ρ, θ and $\dot{\theta}$ is driven by their secular components, which fits very well with the approximations obtained from the indirect method. Interestingly, the secular evolution of ρ have changed from quadratic to linear, justifying the different slopes showed in Figure 2 for $\tau_f\,(\varepsilon)$.

Finally, Figure 7 corresponds to a transfer maneuver in the transition zone, with $\varepsilon = 1.5038\,10^{-7}$, $a = 1.2186\,10^{-6}\,\mathrm{m/s^2}$ and $\tau_f = 5.2442$. The thrust angle profile reflects said transition between both limit cases, taking intermediate values. The radial distance profile is still very similar to the thrust-dominated case, but the trajectory no longer has an overshoot in θ. The curves for $\dot{\rho}$, $\dot{\theta}$ and the costate also present clear differences from the thrust-dominated case, although they have not yet developed the oscillatory behavior which characterizes the gravity-dominated regime.

CONCLUSION

The minimum-time constant-thrust transfer between two close, coplanar circular orbits has been studied, using a non-linear relative motion formulation in curvilinear coordinates and both the direct and indirect methods. Results show the existence of two different regimes depending on whether the maneuver takes less or more than one orbit to complete, with fundamental qualitative differences between them. In the short, or thrust-dominated maneuver the thrust orientation control law is nearly bang-bang along the radial direction. In the long, or gravity-dominated maneuver said control law oscillates with small amplitude about the transversal direction. The ratio of the required radial

displacement and the available thrust is identified as the main parameter of the problem and a clear relation between this parameter and the maneuver time is observed for both regimes. Finally, an approximate analytical study of the Euler-Lagrange equations leads to an explicit expression for the relation between maneuver time, radial displacement and thrust parameter, as well as other qualitative informations about the state and costate. This information can be very useful to construct initial guesses for iterative optimization algorithms or to quickly determine the main characteristics of a continuous-thrust maneuver without actually solving the associated Optimal Control Problem.

ACKNOWLEDGMENT

This work has been supported by the Spanish Ministry of Education, Culture and Sport through its FPU Program (reference number FPU13/05910), and by the Spanish Ministry of Economy and Competitiveness within the framework of the research project "Dynamical Analysis, Advanced Orbital Propagation, and Simulation of Complex Space Systems" (ESP2013-41634-P). The authors also want to thank the funding received from the European Union Seventh Framework Programme (FP7/2007-2013) under grant agreement N 607457 (LEOSWEEP).

REFERENCES

[1] M. Ruiz, E. Ahedo, C. Bombardelli, I. Urdampilleta, M. Merino, and F. Cichocki, "The FP7 LEOSWEEP project: improving Low Earth Orbit Security with Enhanced Electric Propulsion," *Space Propulsion Conference*, 2014.

[2] C. Bombardelli and J. Peláez, "Ion beam shepherd for contactless space debris removal," *Journal of Guidance, Control, and Dynamics*, Vol. 34, No. 3, 2011, pp. 916–920.

[3] J.-P. Marec, *Optimal space trajectories*, Vol. 1. Elsevier, 2012.

[4] C. D. Hall and V. Collazo-Perez, "Minimum-time orbital phasing maneuvers," *Journal of guidance, control, and dynamics*, Vol. 26, No. 6, 2003, pp. 934–941.

[5] M. Massari and F. Bernelli-Zazzera, "Optimization of low-thrust reconfiguration maneuvers for spacecraft flying in formation," *Journal of Guidance, Control, and Dynamics*, Vol. 32, No. 5, 2009, pp. 1629–1638.

[6] J. L. Gonzalo and C. Bombardelli, "Optimal Low-Thrust-Based Rendezvous Maneuvers," *Advances in the Astronautical Sciences*, No. AAS 15-364, Williamsburg, Virginia, USA, AAS/AIAA, January 11-15 2015.

[7] C. Bombardelli, J. L. Gonzalo, and J. Roa, "Compact Solution of Circular Orbit Relative motion in Curvilinear Coordinates," *Advances in the Astronautical Sciences*, No. AAS 15-661, Vail, Colorado, USA, AAS/AIAA, August 9-13 2015.

[8] A. E. Bryson and Y.-C. Ho, *Applied Optimal Control. Optimization, Estimation and Control.* Taylor & Francis, 1975.

[9] J. T. Betts, *Practical Methods for Optimal Control and Estimation Using Nonlinear Programming, Second Edition*. SIAM, 2010.

[10] F. Topputo and C. Zhang, "Survey of Direct Transcription for Low-Thrust Space Trajectory Optimization with Applications," *Abstract and Applied Analysis*, Vol. 2014, Hindawi Publishing Corporation, 2014.

[11] J. L. Gonzalo, "Perturbation Methods in Optimal Control Problems Applied to Low Thrust Space Trajectories," Master's thesis, ETSI Aeronáuticos, Technical University of Madrid (UPM), 2012.

[12] A. Wächter and L. T. Biegler, "On the implementation of an interior-point filter line-search algorithm for large-scale nonlinear programming," *Mathematical programming*, Vol. 106, No. 1, 2006, pp. 25–57.

[13] T. F. Coleman, B. S. Garbow, and J. J. Moré, "Software for Estimating Sparse Hessian Matrices," *ACM Transactions on Mathematical Software*, No. 11, 1985, pp. 363–377.